Journal of Biomolecular NMR, **23:** 195–200, 2002.
KLUWER/ESCOM
© 2002 *Kluwer Academic Publishers. Printed in the Netherlands.*

Accurate measurement of residual dipolar couplings in anisotropic phase

Brian Cutting[a], Joel R. Tolman[a], Steve Nanchen[a] & Geoffrey Bodenhausen[a,b,*]
[a]*Institut de Chimie Moléculaire et Biologique, Ecole Polytechnique Fédérale de Lausanne, BCH, 1015 Lausanne, Switzerland;* [b]*Département de Chimie, Ecole Normale Supérieure, 24 rue Lhomond, 75231 Paris cedex 05, France*

Received 1 March 2002; Accepted 6 June 2002

Key words: quantitative J spectroscopy, residual dipolar couplings

Abstract

The determination of residual dipolar couplings (RDCs) by quantitative J spectroscopy methods such as Heteronuclear Single Quantum Correlation with Phase Encoded Coupling (HSQC-PEC) is prone to systematic errors that may be caused by differential attenuation during the conversion of orthogonal density operator components into observable terms. The attenuation may be caused by miscalibration of radio-frequency pulses and by relaxation effects. A simple method is presented that allows one to remove most of these systematic errors without losses in sensitivity or resolution.

The measurement of one-bond (amide) NH couplings is an essential step for any biomolecular study carried out in anisotropic phase. The relatively large dipolar interaction between the directly bonded nuclei, as well as comparative ease of measurement, makes them a convenient source of orientational constraints. There are now quite a number of different schemes that can be employed to measure these couplings (Tolman and Prestegard, 1996a, b; Tjandra et al., 1996; Ottiger et al., 1998; Yang et al., 1999). These methods may be classified according to whether the coupling is observed as a difference in line frequencies or in the manner of a quantitative J experiment (Vuister and Bax, 1993), where the coupling is encoded in the signal intensity. In general, quantitative J experiments have the advantage of offering high precision of measurement, but may suffer from considerable loss in accuracy if systematic errors are not carefully controlled. For this reason, these methods are most commonly used in situations where precision is critical, for example when protein concentration is low or when the couplings to be measured are small. We discuss here a simple method for the suppression of an important source of systematic error in one particular quantitative J experiment, the HSQC-PEC experiment (Heteronuclear Single Quantum Correlation with Phase-Encoded Couplings) (Tolman and Prestegard, 1996b). The underlying principles are however quite general and should be applicable to a wide range of experiments.

The new method is conceptually based on a constant-time HSQC experiment in which effective $N\text{-}H^N$ couplings (herein the effective couplings are defined as $J_{NH} + \langle D_{NH} \rangle$) are allowed to evolve for the entire constant-time period T. Following this interval, two orthogonal density operator components, $2N_YH_Z$ and N_X, that result from evolution under the $N\text{-}H^N$ coupling are converted into observable proton magnetization. In effect, the couplings are encoded in the *phases* of the corresponding observed proton signals. As one might expect, systematic errors will arise if the conversion of these two 'quadrature' components of the density operator (cosine and sine-modulated according to the evolution under the effective coupling during the time T) into proton magnetization is attenuated in different ways by pulse imperfections and relaxation. Such errors indeed commonly occur, but can be largely suppressed by using two complementary experiments as will be shown in this communication.

The pulse sequence for the HSQC-PEC experiment is shown in Figure 1. At the end of the constant-time

*To whom correspondence should be addressed. E-mail: Geoffrey.Bodenhausen@ens.fr

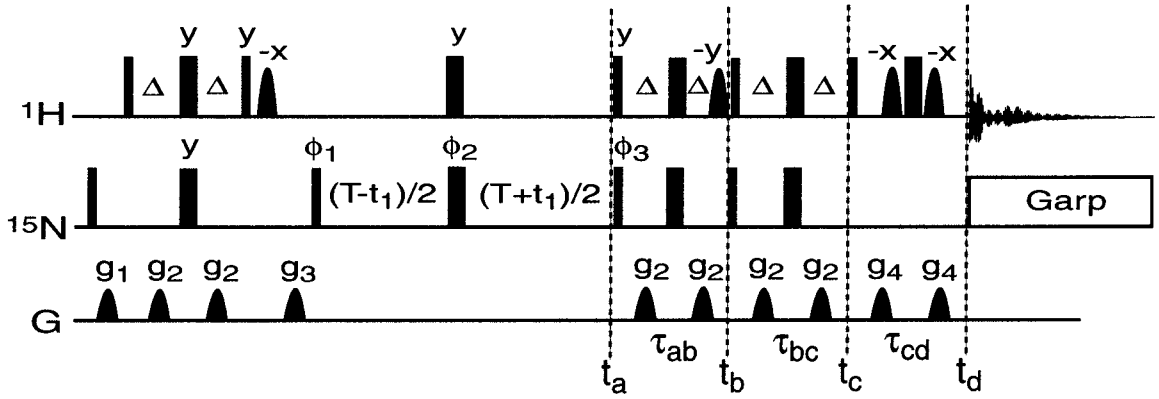

Figure 1. Pulse sequence used for the measurement of effective couplings $J_{NH} + \langle D_{NH} \rangle$. Thin and thick rectangles correspond to $\pi/2$ or π pulses, whereas the shaped pulses at the proton frequency represent 1.2 ms selective 90° Gaussian pulses applied to the water resonance. Gradients, labeled g_1–g_4, were all sine-shaped z-gradient pulses of 1 ms duration with strengths of 7.5, 10, 11, and 23.6 G/cm, respectively. Each interval Δ represents a delay of 2.6 ms ($\approx 1/4J_{NH}$). The constant time delay was either T = 64.516 ms ($T = n_A/J^{nominal}$ with $n_A = 6$ and $J^{nominal} = 93$ Hz) or T = 69.892 ms ($T = n_B/J^{nominal}$ with $n_B = 6.5$). A 4-step phase cycling scheme was employed for each acquired signal: $\phi_1 = \{x, x, x, x\}$, $\phi_2 = \{x, y, -x, -y\}$, $\phi_3 = \{x, x, x, x\}$ and $\phi_{Rec} = \{x, -x, x, -x\}$. Furthermore, for each t_1 increment, 4 signals were acquired and stored separately employing the phases $\phi_1 = \{x, y, x, y\}$ and $\phi_3 = \{x, x, -x, -x\}$ as shown in Table 1. Axial peaks were moved to the edge of the spectrum by simultaneous inversion of the receiver phase ϕ_{Rec} and the phase ϕ_1 on alternate t_1 increments (Marion et al., 1989).

period T, i.e., at time point t_a, the density operator comprises nitrogen coherences $2N_YH_Z$ and N_X that are anti-phase and in-phase with respect to the attached proton, and that are both cosine-modulated by the nitrogen chemical shift as a function of t_1. Corresponding sine-modulated quadrature components also exist, but are omitted here because their theoretical treatment is identical. Conversion of the components of interest, $2N_YH_Z$ and N_X, into observable magnetization is summarized in Equation 1 below for the case in which the phases are $\phi_1 = \phi_3 = x$.

$$\begin{aligned}
\sigma(t_a) &= 2N_YH_Z\cos(\omega_N t_1)\cos(\pi J_{NH}(T) \\
&\quad -N_X\cos(\omega_N t_1)\sin(\pi J_{NH}T), \\
\sigma(t_b) &= H_Y\cos(\omega_N t_1)\cos(\pi J_{NH}T) \\
&\quad -2N_YH_Z\cos(\omega_N t_1)\sin(\pi J_{NH}(T) \\
\sigma(t_c) &= H_Z\cos(\omega_N t_1)\cos(\pi J_{NH}T) \\
&\quad +H_X\cos(\omega_N t_1)\sin(\pi J_{NH}(T), \\
\sigma(t_d) &= H_Y\cos(\omega_N t_1)\cos(\pi J_{NH}T) \\
&\quad +H_X\cos(\omega_N t_1)\sin(\pi J_{NH}T).
\end{aligned} \tag{1}$$

As can be seen in Equation 1, the scheme employed to preserve both terms is reminiscent of commonly employed sensitivity enhancement schemes (Palmer et al., 1991; Kay et al., 1992). From Equation 1 it is clear that the observed proton signals will exhibit a phase that is proportional to the J_{NH} coupling. In order to separate these signals into complementary amplitude-modulated components, as well as to achieve quadrature in t_1, four signals are recorded for each increment of the evolution time t_1. Signals are then pairwise added and subtracted in order to produce two different spectra with signal intensities that are modulated in amplitude by the coupling of interest, as described in Tables 1 and 2.

In this communication, we are concerned with errors introduced by an imperfect conversion of the terms $2N_YH_Z$ and N_X (present at time t_a) into observable terms H_Y and H_X (at time t_d) respectively. The attenuation of these two pathways due to relaxation will not in general be the same. As previously reported (Tolman and Prestegard, 1996b), the differential attenuation of the coherences that occur during the interval 4Δ between times t_a and t_d due to relaxation effects is related to the difference between the rates of longitudinal proton and transverse nitrogen relaxation, the latter being defined as the average between the relaxation rates of the anti-phase and in-phase coherences $2N_YH_Z$ and N_X:

$$\frac{\zeta_{relax}(N_X \rightarrow H_X)}{\zeta_{relax}(2N_YH_Z \rightarrow H_Y)} = \exp\left\{2\Delta\left(R_1^H - R_2^N\right)\right\}. \tag{2}$$

The functions ζ_{relax} represent the fractions of the coherences remaining after consideration of relaxation effects, so that $\zeta_{relax} = 1$ if relaxation can be neglected.

Imperfections in either the ^1H or ^{15}N pulse widths will also affect the two components unequally. Denoting the effects of pulse imperfections using factors f, where $f = 1$ corresponds to perfectly calibrated pulses,

Table 1. Acquisition of four complementary signals, each modulated differently by the heteronuclear coupling constant and by the ^{15}N chemical shift, is achieved by stepping the phases ϕ_1 and ϕ_3

FID number	ϕ_1	ϕ_3	H_Y	H_X
1	x	x	$\cos(\omega_N t_1)\cos(\pi J_{NH} T)$	$\cos(\omega_N t_1)\sin(\pi J_{NH} T)$
2	y	x	$-\sin(\omega_N t_1)\cos(\pi J_{NH} T)$	$-\sin(\omega_N t_1)\sin(\pi J_{NH} T)$
3	x	−x	$\cos(\omega_N t_1)\cos(\pi J_{NH} T)$	$-\cos(\omega_N t_1)\sin(\pi J_{NH} T)$
4	y	−x	$-\sin(\omega_N t_1)\cos(\pi J_{NH} T)$	$\sin(\omega_N t_1)\sin(\pi J_{NH} T)$

Table 2. Post-processing scheme used to recombine the four signals acquired for each t_1 increment in order to form two separate datasets, each modulated as a sine or cosine function of the effective coupling $J_{NH} + \langle D_{NH} \rangle$

FID combinations	Resulting signal	2D spectrum modulated by
1+3	$H_Y \cos(\omega_N t_1)\cos(\pi J_{NH} T)$	$\cos(\pi J_{NH} T)$
2+4	$-H_Y \sin(\omega_N t_1)\cos(\pi J_{NH} T)$	
1−3	$H_X \cos(\omega_N t_1)\sin(\pi J_{NH} T)$	$\sin(\pi J_{NH} T)$
2−4	$-H_X \sin(\omega_N t_1)\sin(\pi J_{NH} T)$	

the resulting effect on the ratio of the two pathways can be expressed approximately in the form

$$\frac{\zeta_{RF}\,(N_X \rightarrow H_X)}{\zeta_{RF}\,(2N_Y H_Z \rightarrow H_Y)} = \frac{\cos\left(\pi\,(1 - f_H)\right)}{\cos\left(\pi\,(1 - f_N)\right)}. \quad (3)$$

How this differential attenuation propagates into a systematic error depends strongly on the magnitude of the effective N-H couplings and the choice of the duration T of the constant-time period. The interval T is typically chosen to be $T = n/J_{NH}^{nominal}$, where n is an integer chosen such that a 'nominal' coupling constant will lead to a signal with a maximum $2N_Y H_Z$ (cosine-modulated) component and a vanishing N_X (sine-modulated) component at time t_a. Couplings that are larger or smaller than this 'nominal' coupling will lead to conversion of a portion of the coherence into the sine modulated component with either a positive or negative coefficient. The choice of n (and hence T) is governed by a compromise between relaxation and the desired resolution. Greater resolution, and thus greater accuracy of determination of the effective N-H couplings, may be achieved by allowing more revolutions of coupling evolution to proceed, i.e., by choosing a larger value of n. This has the effect of amplifying small differences in couplings as the phase increases linearly with T. Note that for a wide frequency distribution of couplings, large values of n may lead to aliasing of the couplings.

The effect of these systematic errors on measured couplings is described in Figure 2. If the coupling is larger than the nominal coupling, $\Delta J = J^{true} - J^{nominal} > 0$, the precessing coherence will acquire an additional phase angle $\Delta\phi_A = \pi \Delta J T$ relative to that expected for the nominal coupling, represented by the departure of the solid vector **A** from the $\langle 2N_Y H_Z \rangle$ axis towards the $-\langle N_X \rangle$ axis. However, due to relaxation or radio-frequency pulse miscalibration, the components may be attenuated to a different extent during their conversion into observable proton magnetization. This is indicated by the dashed vector **A** in Figure 2a, based on the assumption of an attenuation factor $\zeta(N_X \rightarrow H_X) = 0.8$ for the vertical component and an attenuation factor $\zeta(2N_Y H_Z \rightarrow H_Y) = 0.95$ for the horizontal component. In this case the apparent phase $\Delta\phi_A$ gives an *underestimate* of the true coupling. The specific case shown in Figure 2a can be generalised to a distribution of couplings in Figure 2b using Equation 4.

$$J^{app} = J^{nominal} + \frac{1}{\pi T} \tan^{-1}\left(\frac{\zeta\,(N_X \rightarrow H_X)}{\zeta\,(2N_Y H_Z \rightarrow H_Y)} \tan \Delta\phi_A\right). \quad (4)$$

The systematic error is described approximately by a sine function of the difference ΔJ between the true coupling and the nominal coupling. For typical attenuation factors of $\zeta(N_X \rightarrow H_X) = 0.8$ and

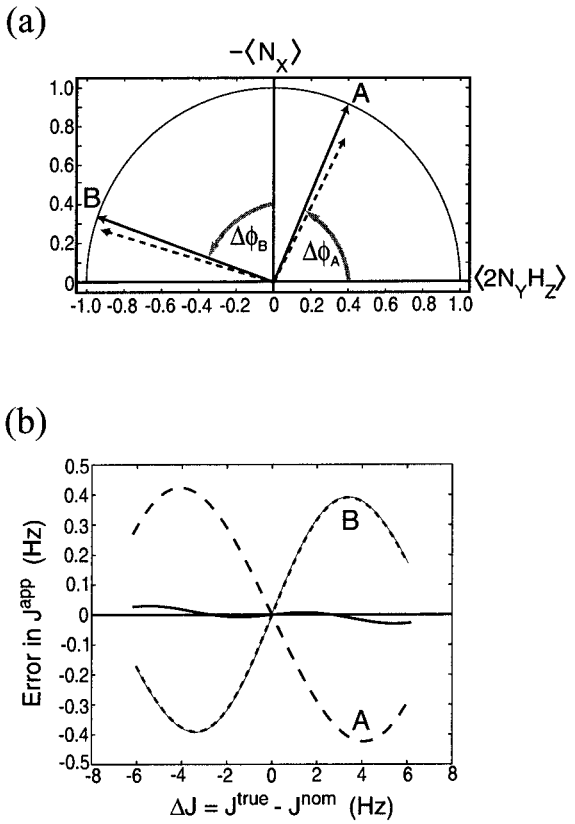

Figure 2. (a) Evolution under the N-H coupling Hamiltonian leads to a precession (assumed counterclockwise although in actual fact J_{NH} is negative) in a two-dimensional space spanned by $\{2N_YH_Z, N_X\}$ with cosine and sine coefficients. This precession proceeds for a constant time T, which is the time required for precession under a nominal coupling to complete $n_A = 6$ half-cycles. The solid vector labelled **A** thus represents precession under an effective coupling that is larger than the nominal coupling, and has precessed through more than 6 half-cycles. The resulting phase angle $\Delta\phi_A$ is proportional to the deviation ΔJ of the true coupling from the nominal value. The angle $\Delta\phi_A$ can be determined from observation of both of the $\langle 2N_YH_Z\rangle$ and $\langle N_X\rangle$ components. In practice, however, the conversion of these components into observable transverse proton magnetization is subject to potentially different attenuating factors, leading to an error in the apparent coupling. The dashed vector is obtained for an attenuation factor $\zeta(N_X \rightarrow H_X) = 0.8$ of the vertical sine component and an attenuation factor $\zeta(2N_YH_Z \rightarrow H_Y) = 0.95$ of the horizontal cosine component. Under these conditions, the apparent phase angle will lead to an underestimate of $\Delta\phi_A$, and hence to an underestimate of the magnitude of the coupling. However, if a second measurement is performed, in which precession (at the nominal coupling frequency) is allowed for an additional quarter cycle ($n_B = 6.5$) and subject to the same attenuation factors, it is seen that the apparent phase angle of the vector **B** will now lead to an overestimate of the true value $\Delta\phi_B$. The error propagated into the measurement depends on the difference ΔJ between the true coupling and the nominal coupling. This is shown in (b) using the same attenuation factors $\zeta(N_X \rightarrow H_X) = 0.8$ and $\zeta(2N_YH_Z \rightarrow H_Y) = 0.95$. It is seen that the error may be considerably reduced by averaging the results obtained in case A with those obtained in case B (i.e., from experiments performed with $n_A = 6$ and $n_B = 6.5$).

$\zeta(2N_YH_Z \rightarrow H_Y) = 0.95$ as shown in Figure 2, the predicted systematic errors in the apparent couplings range between $+0.4$ and -0.4 Hz if $|J^{true} - J^{nominal}| < 15$ Hz. This magnitude will of course vary according to the system studied and the accuracy of the pulse widths.

It is possible to cancel these systematic errors almost completely by performing a complementary experiment. This is done by repeating the experiment identically except that the angle of precession is increased by $\pi/2$ ($n_B = n_A + 0.5$). Note that for even n, the coefficient $\cos(\pi J_{NH}^{nominal} T) = +1$, while for odd n this factor is -1, since the precession illustrated in Figure 2a undergoes n half-cycles. Now for an experiment performed with a half-integral value of n, we expect that a coupling at the nominal frequency will lead to a maximum N_X component and a vanishing $2N_YH_Z$ component. This is illustrated in Figure 2a, for an experiment with $n_B = 6.5$, with the solid vector **B**. The same attenuation factors now result in an *overestimate* in the phase $\Delta\phi_B$, as shown by the dashed vector. The result is that couplings that have been underestimated in experiment A are now overestimated in the complementary experiment B to nearly the same extent. Averaging of the two measurements leads to a significant reduction in the error, as shown by the solid curve in Figure 2b. Although the compensation of the systematic error is not perfect, it is seen that in this case, the error may be reduced to less than 0.03 Hz for $|\Delta J| < 15$ Hz. We refer to this approach as HSQC-PEC[2], for Heteronuclear Single Quantum Correlation with Phase Encoded Couplings and Partial Error Compensation.

One bond N-H^N couplings were measured using the HSQC-PEC[2] experiment at a field of 14.1 T for Ubiquitin dissolved in an approximately 4.5% bicelle solution (30:10:1 DMPC:DHPC:TTAB). Four datasets were acquired in two complementary pairs, with the constant time delay T chosen to be 64.516 or 69.892 ms. The two properly calibrated experiments correspond to the experiments A and B of Figure 2, in which a nominal coupling of 93 Hz leads to $n_A = 6$ and $n_B = 6.5$ half-cycles of precession, respectively. For each of these two-dimensional datasets, 64×1024 complex points were acquired, with spectral widths of 1800 and 8000 Hz respectively, in the ^{15}N and ^{1}H dimensions. An additional pair of datasets (labelled A′ and B′) was acquired under identical conditions with the exception that all ^{15}N pulse widths were deliberately misset to 85% of their optimum value. Figure 3 illustrates dramatically the errors that can arise when

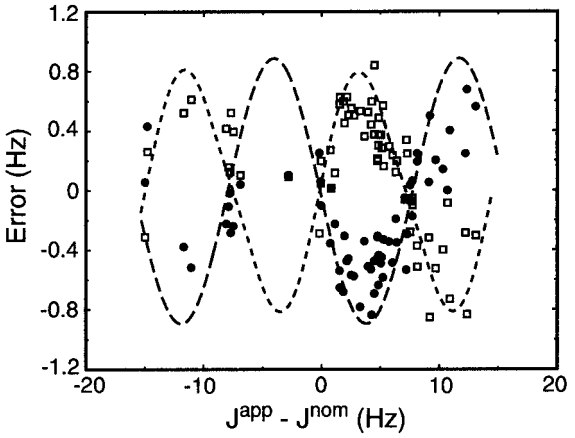

Figure 3. Experimental illustration of the systematic error introduced by differential attenuation of cosine ($2N_YH_Z$) and sine-modulated (N_X) contributions to the signals. The horizontal axis represents the deviation in the apparent coupling from the nominal coupling ($J^{nom} = 93$ Hz), determined from the average of two measurements made with all experimental parameters properly optimized (datasets A and B). The vertical axis represents the errors introduced primarily by miscalibration of the ^{15}N pulse widths. Each filled circle represents the difference between a coupling measured in the 'bad' dataset A′ ($n_A = 6$) and the coupling obtained from the average between the two 'good' datasets, A and B. Analogously, errors in the 'bad' dataset B′ ($n_B = 6.5$) are represented by open squares. For reference, the dashed lines have been added to show the theoretical dependence of the systematic error on the deviation ΔJ of the coupling from its nominal value.

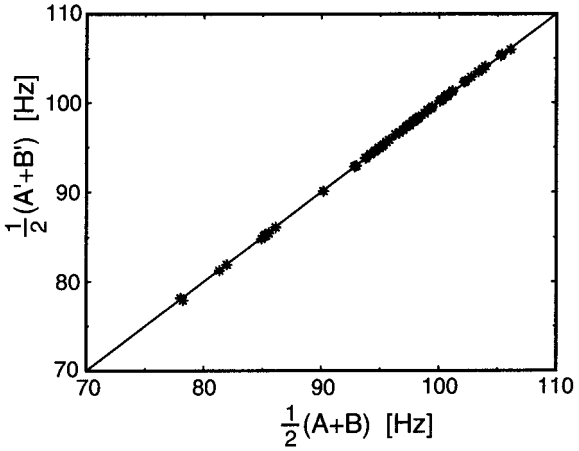

Figure 4. Correlation of the measurements obtained from an average of the apparent couplings of the two 'good' datasets (A and B) and those obtained from an average of the two 'bad' (miscalibrated) datasets (A′ and B′).

cosine ($2N_YH_Z$) and sine (N_X) components are attenuated differentially by miscalibrated pulses. The horizontal axis in Figure 3 corresponds to the best estimates of the couplings determined by averaging of sets A and B, acquired using properly calibrated pulse widths. The vertical axis represents the poor estimates taken from the miscalibrated experiments A′ and B′. As expected from Figure 2, the errors approximately follow a sine function of the deviation of J from $J^{nominal}$. This is demonstrated by superimposing the theoretical sinusoidal error curves of Figure 2 on the datapoints of Figure 3. The location of the nulls in the error curve depend solely on the choice of the duration of the constant-time evolution period T, however the amplitude of the errors depend on several factors. Parameters such as the rates of chemical exchange and relaxation, and the tilt of the effective RF field will vary from residue to residue. If these parameters are assumed to be constant, one would expect simple sinusoidal error curves as indicated by dashed lines in Figure 3. Deviations from the dashed error curves can be ascribed to residue to residue variations in attenuation factors.

An analysis similar to that shown in Figure 3, using the best datasets A and B, indicated that errors were limited to less than 0.1 Hz for almost all residues. That relaxation effects are small in this example is not surprising given the relatively low molecular mass of the protein ubiquitin. Taking the average of the best datasets to represent the 'true' values of the couplings allows us gauge the extent to which the error can be removed. This is shown in Figure 4, where the couplings extracted from the two pairs of experiments are compared. In spite of the large miscalibrations deliberately introduced during the acquisition of sets A′ and B′, it is apparent that the couplings obtained from these poor data are in very good agreement with the 'true' values (RMSD = 0.09 Hz). Residual discrepancies between the two are on the order of the random error.

We have shown that systematic errors arising from differential attenuation of the two orthogonal signal pathways can be largely suppressed by using the HSQC-PEC^2 approach. This simply requires the acquisition of complementary pairs of spectra, differing only in the choice of the duration of the constant-time period. In most cases, this will not require an increase in experimental acquisition time because two complementary experiments, each of half the total experimental duration, can be acquired while maintaining the same resolution in the indirect dimension. This can be accomplished without loss of sensitivity because the final results are averaged. Frequency domain methods for the measurement of couplings may be less prone to systematic errors. However, the high precision obtained per unit time that is characteristic of

quantitative J type experiments makes it worthwhile to minimize their susceptibility to systematic errors. The optimal choice of experiment depends on the specific circumstances.

It should be noted that other relaxation-induced systematic errors, which enter during the constant-time period T (Tolman and Prestegard, 1996b), are not removed by our procedure. It is conceivable that such errors, in addition to those considered in this work, might be compensated by performing additional pairs of experiments using constant time periods differing from those utilized here. For the present work, it is assumed that the uncompensated errors will remain constant between aligned and unaligned systems and will therefore cancel when dipolar couplings are extracted from the difference. Relaxation-induced errors will become more significant as the molecular mass increases, so that the cancellation of these errors will become increasingly important.

Acknowledgements

This work was supported by the Fonds National de la Recherche Scientifique (FNRS), by the Commission pour la Technologie et l'Innovation (CTI) of Switzerland, and by the Centre National de la Recherche Scientifique (CNRS) of France. We are grateful to Heiko Skusa and the research group of Professor Kai Johnsson for valuable assistance with the sample manipulations.

References

Kay, L.E., Keifer, P. and Saarinen, T. (1992) *J. Am. Chem. Soc.*, **114**, 10663–10665.

Marion, D., Ikura, M., Tschudin, R. and Bax, A. (1989) *J. Magn. Reson.*, **85**, 393.

Ottiger, M., Delaglio, F. and Bax, A. (1998) *J. Magn. Reson.*, **131**, 373–378.

Palmer III, A.G., Cavanagh, J., Wright, P.E. and Rance, M. (1991) *J. Magn. Reson.*, **93**, 151–170.

Tjandra, N., Grzesiek, S. and Bax, A. (1996) *J. Am. Chem. Soc.*, **118**, 6264–6272.

Tolman, J.R. and Prestegard, J.H. (1996a) *J. Magn. Reson.*, **B112**, 269–274.

Tolman, J.R. and Prestegard, J.H. (1996b) *J. Magn. Reson.*, **B112**, 245–252.

Vuister, G.W. and Bax, A. (1993) *J. Am. Chem. Soc.*, **115**, 7772–7777.

Yang, D.W., Venters, R.A., Mueller, G.A., Choy, W.Y. and Kay, L.E. (1999) *J. Biomol. NMR*, **14**, 333–343.